X-690-71-42
PREPRINT

NASA TM X- 65474

MULTIPLE EARTH BOW SHOCK CROSSINGS AT LARGE GEOCENTRIC DISTANCES

B. BAVASSANO
F. MARIANI
U. VILLANTE
N. NESS

FEBRUARY 1971

GSFC — GODDARD SPACE FLIGHT CENTER
GREENBELT, MARYLAND

X-690-71-42

MULTIPLE EARTH'S BOW SHOCK CROSSINGS

AT LARGE GEOCENTRIC DISTANCES

B. Bavassano
F. Mariani*
U. Villante

Laboratorio Plasma nello Spazio - C.N.R.
Istituto di Fisica - Università
Roma, Italy

and

N. F. Ness
Laboratory for Extraterrestrial Physics
NASA-Goddard Space Flight Center
Greenbelt, Maryland

February 1971

* - Now, also, Istituto di Fisica - Università - L'Aquila.

X-690-71-42

MULTIPLE EARTH'S BOW SHOCK CROSSINGS

AT LARGE GEOCENTRIC DISTANCES

B. Bavassano
F. Mariani*
U. Villante

Laboratorio Plasma nello Spazio - C.N.R.
Istituto di Fisica - Università
Roma, Italy

and

N. F. Ness
Laboratory for Extraterrestrial Physics
NASA-Goddard Space Flight Center
Greenbelt, Maryland

February 1971

* - Now, also, Istituto di Fisica - Università - L'Aquila.

Abstract

A series of very distant earth's bow shock crossings has been identified by the magnetic field experiment on board Pioneer 8 at geocentric distances between 120 and 200 R_E, during the period December 19 to 25, 1967. The normal to the shock is generally found lying in or very near the ecliptic plane, at an average angle of 70° with respect to the earth-sun line. The average ratio of field magnitudes on the interplanetary and the magnetosheath sides of the bow shock is very near to 2. The location of these crossings is consistent with that expected from the Dryer and Heckman computations of the distant bow shock configuration, when the aberration of the solar wind is taken into account. The shock is also aligned with the configuration extrapolated from the Explorer 33 observations which extend only to 75 R_E. Our conclusion is that a well-developed bow shock is still observed at these very large distances. The intermittent observations are interpreted as an effect of the sweeping back and forth of the shock across the spacecraft orbit, due to time variations of the solar wind.

PRECEDING PAGE BLANK NOT FILMED

1. Introduction.

The characteristics of the magnetosphere and the geomagnetic tail, as well as the location and the motions of the earth's bow shock have been extensively studied in the past several years. Most of the observations are limited to geocentric distances less than 40 R_E (1 R_E = earth's radius). However, the bow shock and tail observations by Explorers 33 and 35 have shown that the tail is still an ordered structure, similar to that observed near the earth, out to 80 R_E, well beyond the lunar orbit (see review by Ness, 1969). An ordered structure in the antisolar direction has been sporadically observed by Pioneer 8 at ~500 R_E (Mariani and Ness, 1969) and by Pioneer 7 at ~1000 R_E (Ness et al., 1967 and Fairfield, 1968). As regards the bow shock, it has been directly observed onboard Explorer 33 up to a maximum geocentric distance of 75 R_E (Behannon, 1968).

It is the purpose of this paper to discuss a series of well defined bow shock crossings by Pioneer 8, at geocentric distances between 120 and 200 R_E. In section 2 a short summary of the instrument characteristics and the trajectory are given. The experimental observations are shown in section 3, where they are also compared with theoretical predictions. In the last section, the results are discussed.

2. Instrumentation and Trajectory

The magnetic field experiment on Pioneer 8 consists of a monoaxial fluxgate sensor, similar to those used on the Pioneer 6 and 7 space probes (Scearce et al., 1968). The only difference on Pioneer 8 was the use of a dual range, automatically switched system. The high range was $\pm 96\gamma$ and the low range $\pm 32\gamma$ with sensitivities corresponding to 8-bit digitization, respectively, of $\pm 0.375\gamma$ and $\pm 0.125\gamma$. All data used in the present paper have been obtained while operating in the low range.

The spin period of the spacecraft was 1.0 second and individual vector measurements were spin synchronized. However, due to telemetry synchronization of the data transmission, not all available data could be telemetered, which implies they are not equally-spaced in time. The average time interval between successive determinations of $\underline{B}$ is 1.5 seconds during the period of interest.

The Pioneer 8 spacecraft was launched on 13 December 1967 at 14 h 08 m UT. Aphelion and perihelion of the orbit were respectively 1.088 and 0.9892 AU; the inclination of the orbital plane to the ecliptic plane was 0.0578 degrees; the orbital period was 386.6 days. The trajectory for the first 18 days as projected on the ecliptic plane is shown in Figure 1; the distance of the spacecraft from the ecliptic, i.e., Z_{SE} distance, was never greater than 5.2 R_E.

3. Experimental Observations.

The identification of distant bow shock crossings by Pioneer 8 using only magnetic field data, was based on the observation of an abrupt field magnitude discontinuity accompanied by a simultaneous increase in the short period field fluctuations. The field observations were afterwards tested to verify whether or not the jump conditions, which must be satisfied by the magnetic field at a shock, are fulfilled.

Several tens of such shock crossing events were observed in the first two weeks of the Pioneer 8 flight. An example is shown in Figure 2 using thirty-second averages of the field elements for the days December 22 and 23, 1967. $\overline{F}$, θ and ϕ are the field magnitude, the inclination to the ecliptic and the azimuth on the ecliptic with respect to the direction of the sun. Also shown is the Pythagorean mean variance $\delta = \left[\delta_x^2 + \delta_y^2 + \delta_z^2\right]^{1/2}$ where δ_x, δ_y and δ_z are the 30 second variances of the individual field components with an average sample interval of 1.5 seconds. This means approximately 20 data points were used to construct each component average and each variance.

At 1918 UT of December 22, the field intensity abruptly increased by a factor of two and then a few minutes later at 1922 UT returned back to the original value; during this time interval the variance, δ, is considerably higher than before and after. This behaviour is interpreted as a crossing of the shock; the first field discontinuity occurs when the spacecraft is located in the interplanetary medium and enters the magnetosheath. The field is compressed and the high frequency fluctuations typical of the magnetosheath are observed. The second discontinuity

represents the reverse crossing from the magnetosheath into the interplanetary medium. A similar situation occurs again at 1940 UT and multiple bow shock crossings are seen to occur for many hours afterwards. After 2100 UT, until 0500 UT of the next day December 23, several other events of the same kind are systematically observed.

As a whole, in the period from December 19 to December 25, 1967 more than thirty events have been selected and interpreted as possible shock crossings. The first exit of the spacecraft into the interplanetary medium occurred on 18 December 1967. However, due to the perturbation associated with an SSC observed at 0538 December 18 on the ground, it is almost impossible to identify the exact time. The first clear outbound shock crossing occurs at 2208 UT when a decrease of the field by a factor of two occurred, followed by a period of steady field.

The possibility that what is observed is actually a field structure already existing in the interplanetary medium and convected past the Pioneer 8 orbit can be ruled out by comparison with simultaneous magnetic field data collected by Explorer 35. The trajectory of this satellite is shown in Figure 1 for the days following December 21, 1967 (prior to this, Explorer 35 was inside the magnetosphere). The Explorer 35 spacecraft is in a very favorable location since the solar plasma sweeping past the Explorer 35 position also sweeps past the Pioneer 8.

Figure 3 shows the hourly field averages observed by Explorer 35 (a) and Pioneer 8 (b), by means of the usual parameter set $\overline{F}$ and $\overline{\overline{F}}$, Θ, ϕ, defined in the caption. If the time delay of the field convected toward Pioneer 8 is ta into account (assuming a plasma velocity =400 km/sec implies, for days

22 to 25, a delay from ~25 to ~50 minutes), one concludes that the field observed by the two spacecraft is very similar, except in the time intervals when Pioneer 8 bow shock crossings have been identified. During these occasions the field magnitude detected by Pioneer 8 is distinctly higher than that observed by Explorer 35. Thus, the high field observed at the Pioneer 8 location does not represent an interplanetary field structure: the compressed field is a local effect.

Careful comparison of the hourly average data in the days following December 25 also shows several other shorter time intervals in which the field magnitude observed by Pioneer 8 is higher than that observed by Explorer 35. According to the previous interpretation this might correspond to other bow shock crossings. However, examination of the 30 sec averages of the field elements does not allow a clear identification. Final re-entry of the spacecraft into the magnetosheath could not be unambigously identified after 25 December.

All the shock crossings observed in the period December 19 to 25 have been studied in detail. Average magnetic field vectors immediately before and after the field discontinuity have been computed. An appropriate smoothing of the field fluctuations was obtained, in each case, by taking averages over time intervals of appropriate length, 30 to 300 seconds. The orientation of the shock normal $\underline{N}$ was computed by means of the coplanarity theorem (Colburn and Sonett, 1966). A plot of the angles θ_N and ϕ_N, is given in Figure 4. In most of the cases the estimated errors on the angles θ and ϕ is about $\pm 20^{\circ}$.

Methods have been worked out to improve significantly the determination of the shock normal orientation(Chao, 1970; Lepping and Argentiero, 1970).

However, they are based on the simultaneous knowledge of both magnetic and plasma data. In our computations based on the knowledge only of the magnetic field, it has been impossible either to use the above improved methods or to check the complete set of the Rankine-Hugoniot conditions. However, a check has been made on the tangential field component, whose orientation cannot be changed through the shock. A different sort of check has been made looking at the statistical properties of the available parameters for the complete set of shock crossing to check that they. as a whole, satisfy the expected relationships for the distant bow shock (Dryer and Heckman, 1967).

4. Discussion.

The locations of the bow shock crossings we have found are shown in Figure 1, where the theoretical shape of the bow shock, as predicted by Dryer and Heckman (1967), is also drawn. With a 4 to 6 degree aberration taken into account, the expected and the observed locations match quite well. The computations have been made with a magnetosonic Mach number 3.8 and specific heat ratio $\gamma = 1.2$, so that some discrepancies could be expected. Both the above figures are rather small. Since the effects of their increase are opposite (Spreiter et al., 1965) the configuration of the shock should still be well described.

The multiple observations of the bow shock are probable due to its motion, as well as to its possible oscillation. Since the trajectory of the spacecraft is practically tangential to the average position of the theoretical bow shock, this tends to sweep the shock back and forth across the probe with only slight variations in upstream interplanetary conditions. An estimate of the average position of the bow shock can be obtained from the ratio of the time spent by the spacecraft in the interplanetary medium to that spent in the magnetosheath. During the days of observations this ratio is much higher than 1, which means that the boundary is nearer to the antisolar direction than estimated by the simple observation of the crossing positions.

The expected orientation of the normal on the ecliptic plane as derived by Figure 1 is about $\phi_{SE} = 290^{\circ}$ or 70° with respect to the earth-sun line. This orientation fits satisfactorily with the observed average, as shown in Figure 4. Although most of the observations indicate that the inclination θ_N is near to zero, there is a significant number of cases when θ_N is greater than ± 30 degrees. Generally, in these cases the variation

of the magnetic field direction across the shock is small, from which it follows that the normal determination can be in error by more $\pm 20^\circ$. If these larger values of Θ_N are considered physically significant, they may be interpreted as an effect of local deformation of the bow shock, as well as of a really different inclination of the solar wind flow to the ecliptic plane.

Other possible checks can be made on the ratios of the magnitudes as well as on the changes of direction of the magnetic field on the two sides of the bow shock. Theoretical relationships, as derived from the Rankine-Hugoniot conditions, are (Smit, 1967):

$$\tan \lambda_1 = \frac{M^2 \tau^2 (1+S^2)\left[\bar{\rho}\tau(1+S\tau)-(\tau-S)\right] - Q\bar{\rho}S(1+\tau^2)(\tau-S)^2}{M^2\tau^2(1+S^2)\left[\bar{\rho}(1+S\tau)+\tau(\tau-S)\right] - Q\bar{\rho}(1+\tau^2)(\tau-S)^2} \qquad (1)$$

$$\left(\frac{B_1}{B_0}\right)^2 = \frac{1}{(1+\tau^2)(1+S^2)}\left\{(\tau-S)^2 + \left[\frac{\bar{\rho}(1+S\tau)M^2\tau^2(1+S^2)-Q(\tau-S)^2}{M^2\tau^2(1+S^2)-Q\bar{\rho}(\tau-S)^2}\right]^2\right\} \qquad (2)$$

Figure 5(a) shows the upstream (subscript 0) and downstream (subscript 1) quantities in the plane of the field $\vec{B}$ and the shock normal $\vec{N}$. The angles λ_0, λ_1 and δ are counted positive in the anticlockwise direction, the other angles in clockwise direction. The other parameters are defined as follows:

$$S = \tan \lambda_0 \qquad \tau = \tan \delta \qquad \bar{\rho} = \frac{\rho_1}{\rho_0}$$

$$a_0^2 = \gamma \frac{p_0}{\rho_0} \qquad b_0^2 = \frac{B_0^2}{4\pi\rho_0^2} \qquad Q = \frac{b_0^2}{a_0^2} \qquad M = \frac{V_0}{a_0}$$

where a_o is the upstream sound velocity, b_o the upstream Alfven velocity, ρ_o and p_o respectively the upstream density and pressure, γ the gas constant V_o the solar wind velocity and M the sonic Mach number.

Figure 5(b) shows the relative orientations ψ_o and ψ_1 of the field vector with respect to the bow shock, respectively in the interplanetary medium and in the magnetosheath. Several curves are drawn for different values of the sonic Mach number M and for $\gamma = 5/3$ and Q = 0.6. The angle α between the solar wind flow and the normal to the shock is taken equal to 70^o (which corresponds to $\phi_{SE} = 290^o$).

The ratio β between thermal and magnetic pressures is taken equal to 2. The observed pairs of ψ_o and ψ_1 are also indicated. The agreement is satisfactory and indicates the values of M between 5 and 8 are appropriate. As regards the field magnitudes, figure 5(c) gives the theoretical behavior of $\frac{|B_1|}{|B_o|}$ as a function of the angle ψ_o. In this case the observed ratios also match the theoretical curves corresponding to the interval M = 5 to 8. These results are consistent with the actual solar wind Alfvén Mach number distribution and in excellent agreement with the sonic Mach number distribution derived from IMP-4 observations by Fairfield (1970).

Thus, all the evidence obtained from the Pioneer 8 magnetic field observations indicates that the bow shock is still well-defined at geocentric distances up to about 200 R_E, although motions and oscillations may play an important role in the detailed time sequence of observations.

Further support to the above conclusions also comes from visual inspection of the plots of the magnetic field observed by Pioneer 7 in the region where its trajectory was very near to that of Pioneer 8 (Figure 1). Several features similar to those shown in Figure 2 are present in these plots. A detailed analysis of all the available Pioneer 7 magnetic field data is planned.

5. Conclusions.

The experimental observation of the geometric configuration of the bow shock and of its temporal variation at large geocentric distances is an important task for a better knowledge of the solar wind interaction with the geomagnetic field in the antisolar region.

The observations by Pioneer 8 show the existence of a well-defined bow shock structure up to geocentric distances of about 200 R_E. The observed angle of the shock normal with respect to the earth-sun line was about 70 degrees, which yields a Mach angle of 20°. The bow shock was moving or oscillating and, due to the small angle of the spacecraft trajectory with respect to the bow shock, a large number of crossings was observed on board Pioneer 8. The magnitude and directional changes of the magnetic field corresponding to the crossings are in good agreement with those theoretically expected. Since the time spent in the interplanetary medium is more than that spent inside the magnetosheath, the actual boundary should be somewhat nearer to the axis of the magnetospheric tail than estimated by observations. The behavior of the magnetic field following December 25, 1967 is such that the existence of a well defined bow shock is strongly suggested at distances beyond 200 R_E.

These observations indicate that the disturbed solar wind region trailing behind the earth (and other planets with bow shocks) extends to great distances. Hence interpretations of other data obtained in such regions must consider such effects. The data also suggest that planetary flyby missions in the future may be able to indirectly examine the solar wind - planet interaction and the nature of the planetary ionosphere or magnetic field even at large distances, if suitably located aftward of the target planet relative to the solar wind flow.

Acknowledgements

The authors gratefully acknowledge fruitful discussion with Dr. K. Schindler of ESRIN. Thanks are also due to Mr. C. S. Scearce of the NASA-Goddard Space Flight Center and Dr. S. Cantarano of the Rome group for their help in the engineering development of the instrument.

We also appreciate discussion of these results with Drs. L. F. Burlaga and D. H. Fairfield.

Figure Captions

Figure 1 Projection on the ecliptic plane of the Pioneer 8, Explorer 35 and Pioneer 7 orbits. Bars across the Pioneer 8 orbit indicate the location of the observed bow shock crossings. Also shown are the distant shock and magnetopause configurations observed by Explorer 33 (Behannon, 1968) and the ideal non-aberrated configuration of the shock as computed by Dryer and Heckman (1967) for a magnetosonic Mach number $M_M = 3.8$ and $\gamma = 1.2$.

Figure 2 Thirty-second averages of the magnitude $\overline{F}$, inclination with respect to the ecliptic θ (+North,-South) and azimuth in the ecliptic ϕ(ϕ=0° toward the sun and rotates counterclockwise) of the magnetic field observed by Pioneer 8 in 22-23 December 1967. On the top, the Pythagorean mean variance.

Figure 3 Hourly averages of the magnetic field elements, ($\overline{F}$, computed from the average field components; $\overline{\overline{F}}$, computed from the individual magnitudes) observed onboard Explorer 35 (a) and Pioneer 8 (b) from 22-31 December.

Figure 4 Inclination with respect to the ecliptic θ_N (+North, -South) and azimuth in the ecliptic ϕ_N ($\phi_N = 0^\circ$ toward the sun and rotates counterclockwise) of the normal to the shock surface for the analyzed crossings. The expected and the computed average value of ϕ_N are also shown.

Figure 5 a) The definition of the shock parameters (upstream, subscript o; downstream, subscript 1),

b) The relationship between the angles ψ_o and ψ_1 of the magnetic field vectors on the two sides of the shock. Several curves are shown, computed for a range of Mach numbers and for $\alpha = 70^o$, $\beta = 2$ and $\gamma = 5/3$. The dots are the observed values.

c) The ratio of the field magnitude $|B_1|$ inside the magnetosheath to that in the interplanetary space $|B_o|$, as a function of the angle ψ_o.

References

Behannon, K. W., Mapping of the earth's bow shock and magnetic tail by Explorer 33, J. Geophys. Res., 73, 907, 1968.

Chao, Jih Kwin, Interplanetary Collisionless Shock Waves, MIT-CSR TR-70-3, February 1970.

Colburn, D. S., C. P. Sonett, Discontinuities in the solar wind, Space Sci. Rev., 5, 439, 1966.

Dryer, M. and G. R. Heckman, On the hypersonic analogue as applied to planetary interaction with the solar plasma, Planet. Space Sci., 15, 515, 1967.

Fairfield, D. H., Simultaneous measurements on three satellites and the observation of the geomagnetic tail at 1000 R_E, J. Geophys. Res., 73, 6179, 1968.

Fairfield, D. H., Average and unusual locations of the earth's magnetopause and bow shock, NASA-GSFC preprint X-692-70-452, 1970.

Lepping, R. P., and P. D. Argentiero, Improved Shock normals obtained from combined magnetic field and plasma data from a single spacecraft, NASA-GSFC preprint X-692-70-276, 1970. J. Geophys. Res., in press.

Mariani, F and N. F. Ness, Observations of the geomagnetic tail at 500 Earth radii by Pioneer 8, J. Geophys. Res., 74, 5633, 1969.

Ness, N. F., The geomagnetic tail, Revs. Geophys., 7, 97, 1969.

Ness, N. F., C. S. Scearce and S. Cantarano, Probable observations of the geomagnetic tail at 6 x 10^6 kilometers by Pioneer 7, J. Geophys. Res., 72, 3769, 1967.

Scearce, C. S., C. H. Ehrmann, S. Cantarano and N. F. Ness, Magnetic field experiment Pioneers 6, 7 and 8, NASA-GSFC preprint X-616-68-370, 1968.

Smit, G. R., Bow shock parameters in different flow normalizations, ESRO SN-17 (ESRIN), 1967.

Spreiter, J. R., A. L. Summers and A. Y. Alksne, Hydromagnetic flow around the magnetosphere, Planet. Space Sci., 14, 223, 1965.

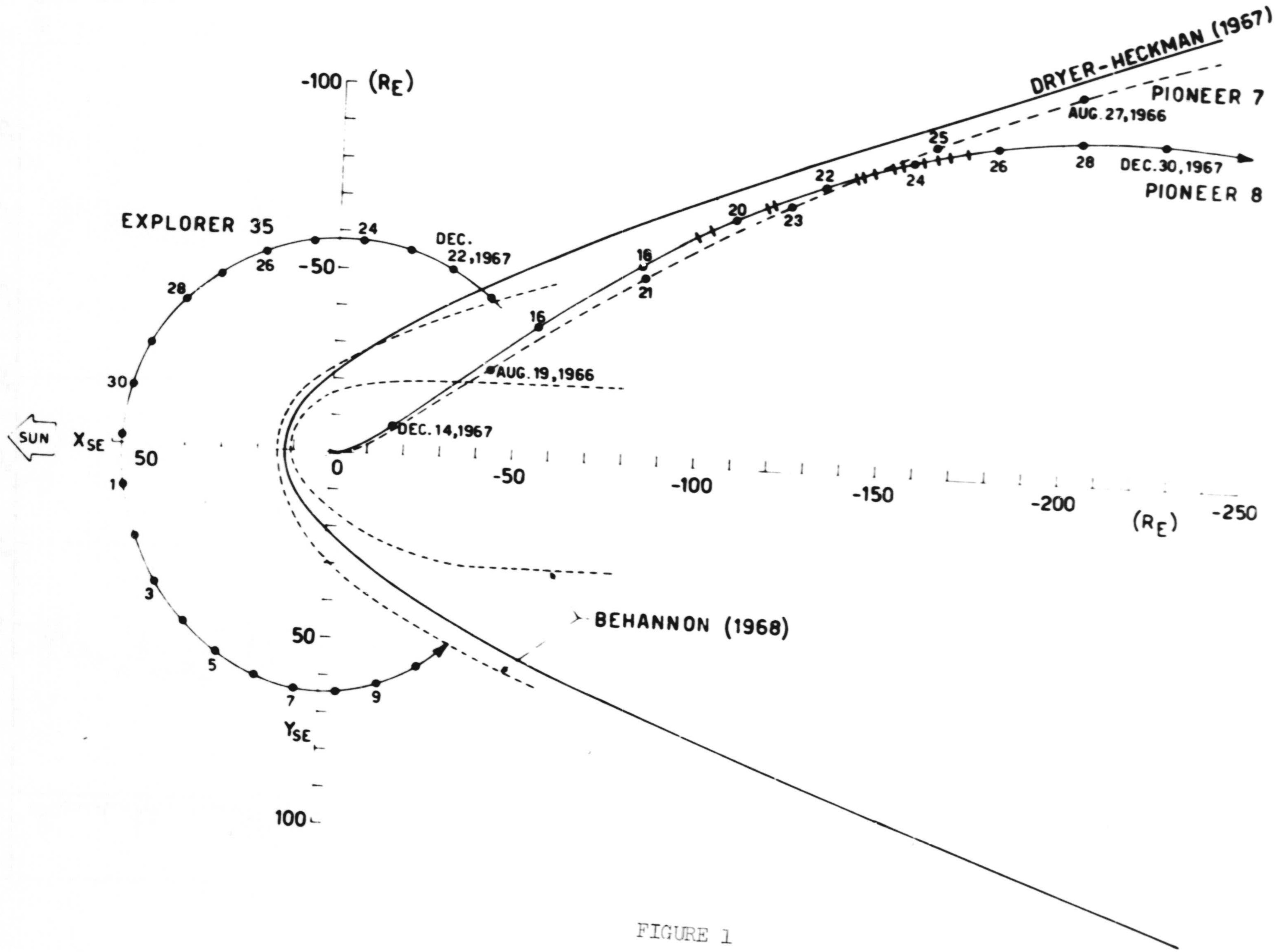
DRYER-HECKMAN (1967)
PIONEER 7
AUG. 27, 1966
PIONEER 8
DEC. 30, 1967
EXPLORER 35
DEC. 22, 1967
AUG. 19, 1966
DEC. 14, 1967
BEHANNON (1968)
SUN
X_{SE}
Y_{SE}
(R_E)
-100
-50
0
50
100
-150
-200
-250

FIGURE 1

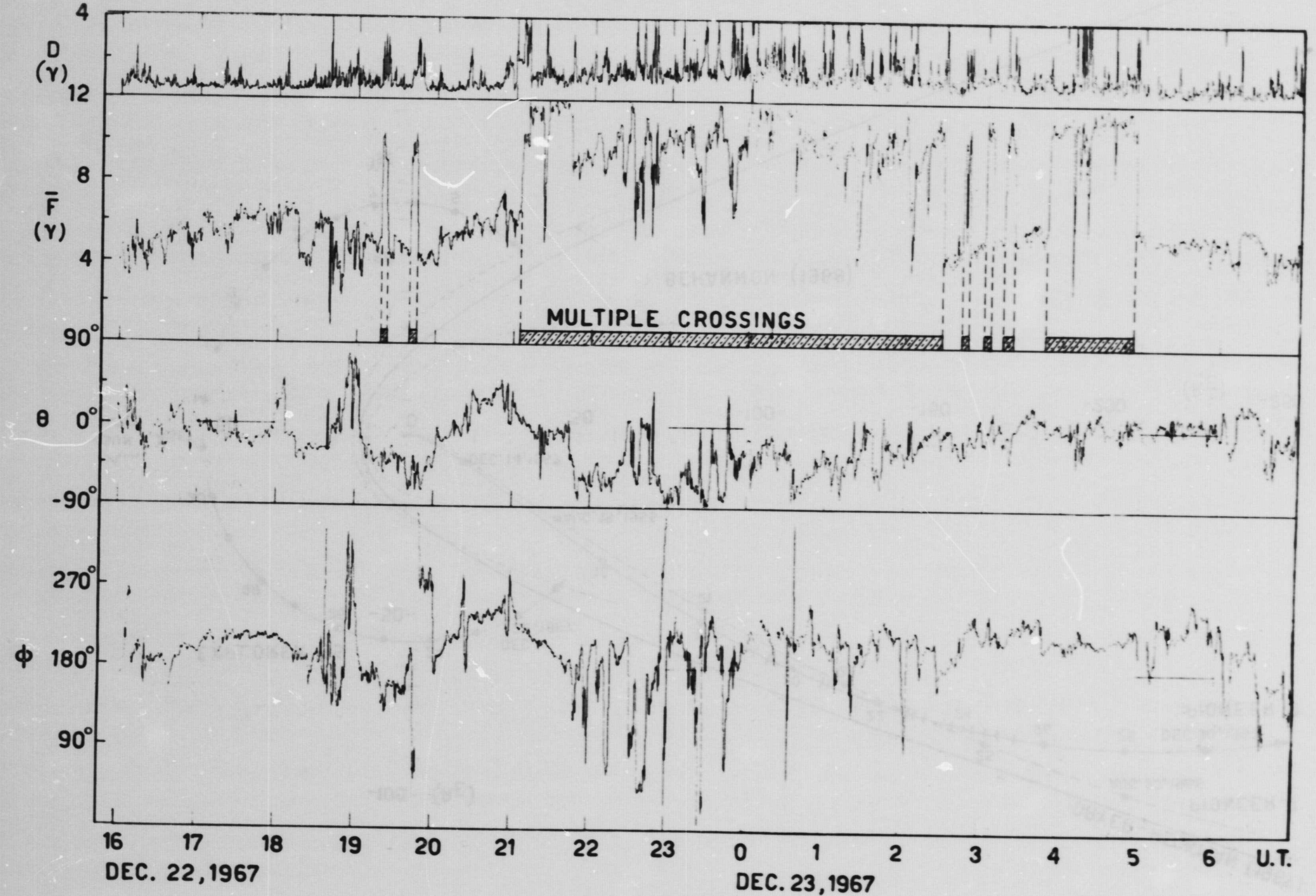

D
(γ)
4
12
F̄
(γ)
8
4
MULTIPLE CROSSINGS
θ
90°
0°
-90°
φ
270°
180°
90°
16
17
18
19
20
21
22
23
0
1
2
3
4
5
6
U.T.
DEC. 22,1967
DEC. 23,1967

FIGURE 2

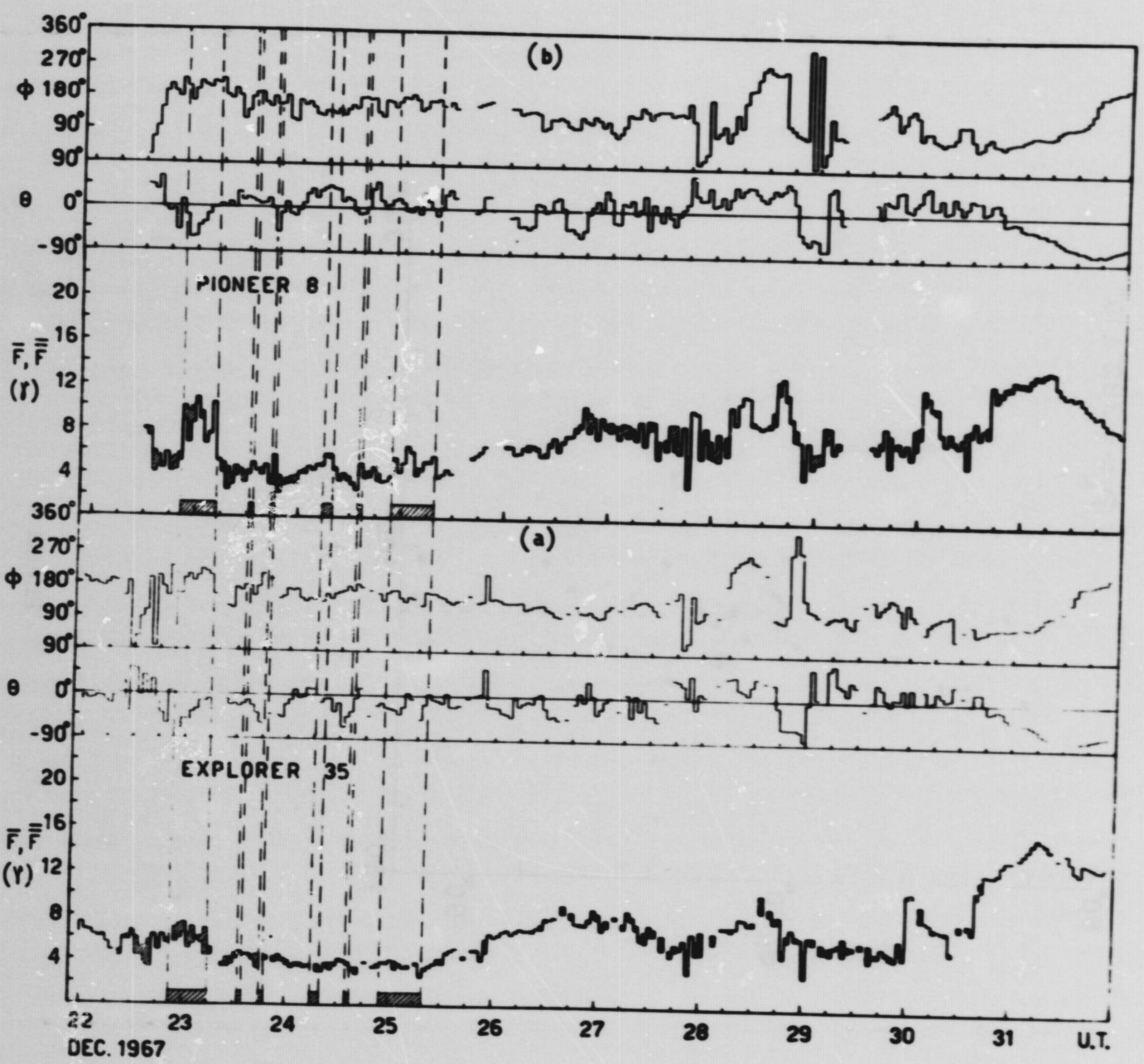

FIGURE 3

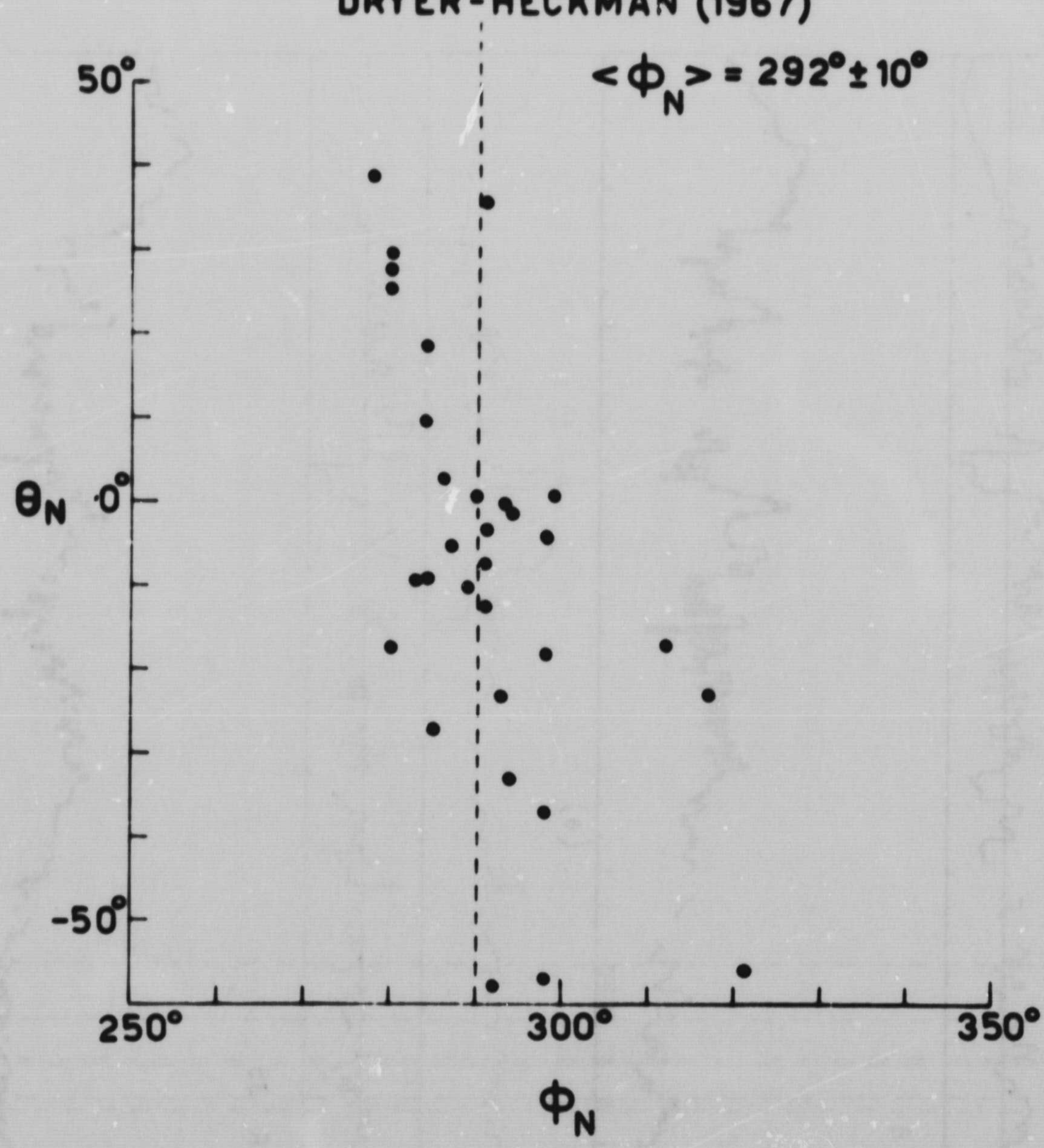

DRYER-HECKMAN (1967)
$<\phi_N> = 292° \pm 10°$
50°
0°
-50°
θ_N
250°
300°
350°
ϕ_N

FIGURE 4

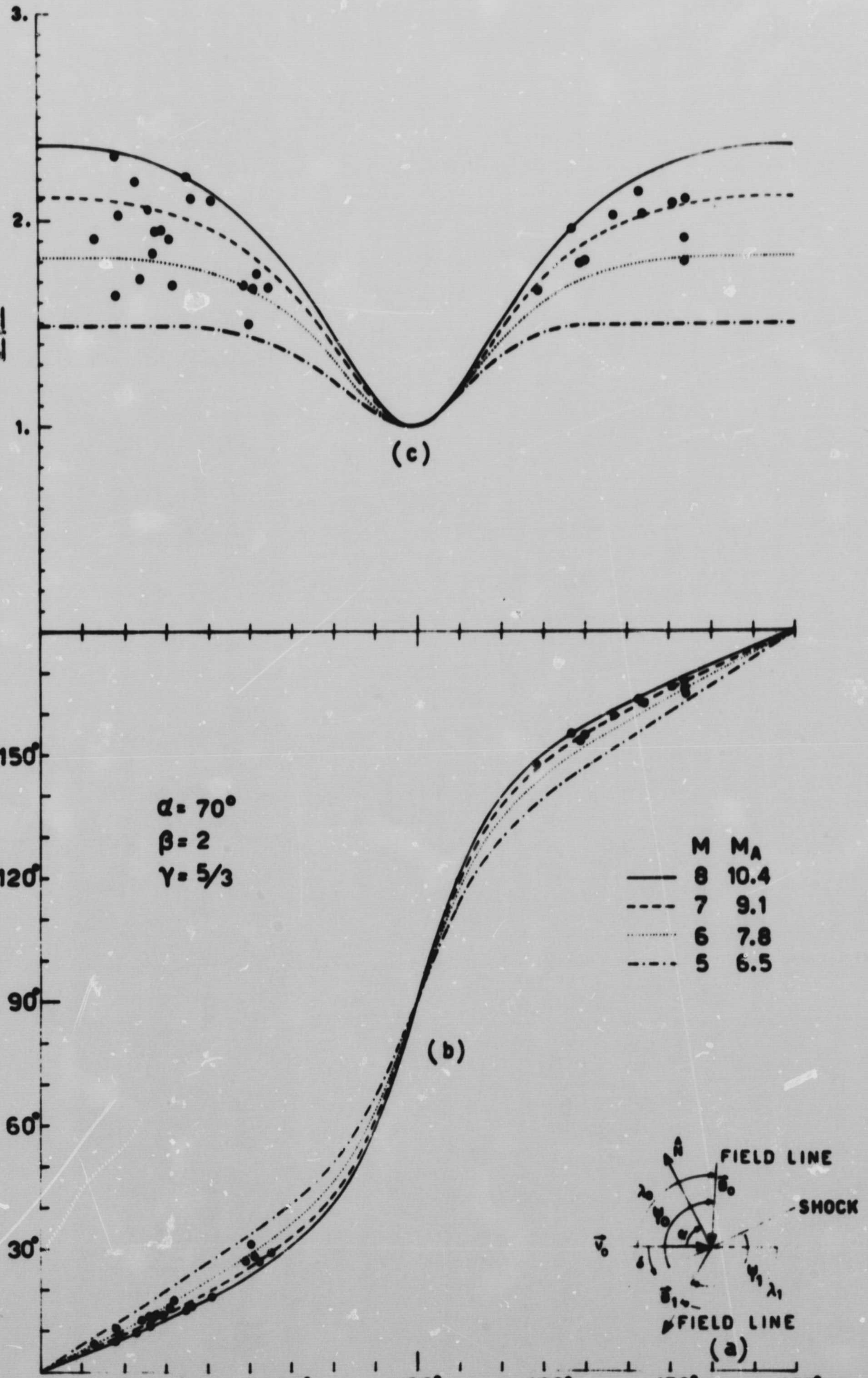

3.
2.
1.
$\frac{|B_1|}{|B_0|}$
(c)
150°
120°
90°
60°
30°
ψ_1
$\alpha = 70°$
$\beta = 2$
$\gamma = 5/3$
M M_A
8 10.4
7 9.1
6 7.8
5 6.5
(b)
FIELD LINE
SHOCK
FIELD LINE
(a)
30° 60° 90° 120° 150° 180°
ψ_0

FIGURE 5